JOURNAL OF MECHANICAL ENGINEERING AND SCIENCES (JMES)
ISSN: 2289-4659 e-ISSN: 2231-8380
VOL.14, ISSUE 1, 6380 – 6392
DOI: https://doi.org/10.15282/jmes.14.1.2020.14.0499

ORIGINAL ARTICLE

Study on numerical analysis of dynamic parameters of mobile walking robot

Mikhail Polishchuk[1], Mykyta Suyazov[1] and Mark Opashnyansky[1]

Department of Technical Cybernetics, Igor Sikorsky Kyiv Polytechnic Institute, 03056 Kyiv, Ukraine. Phone: +380503555777

ABSTRACT – A dynamic model of a walking robot is proposed for moving along surfaces of different topologies and orientations to the horizon. The principal difference between walking robot mechanisms is that they are made in the form of flexible pedipulators. Actually the pedipulators are a set of spherical rings with a hydraulic or pneumatic drive. The patented design (Patent UA No 117065, publ. 2018.06.11) of the robot's feet is anthropomorphic and allows the robot to work in the angular coordinate system inherent in the human walking machine. The proposed mathematical model allows us to calculate the dynamic parameters (forces and moments) and compare these parameters with the allowable technological load that a walking robot can perform without losing adhesion with the displacement surface.

ARTICLE HISTORY
Revised: 21st Sept 2019
Accepted: 21st Sept 2019

KEYWORDS
mobile robots;
stepping mechanisms;
pedipulators;
robots of vertical movement.

INTRODUCTION

Unlike stationary and transport industrial robots, mobile robots have the ability to navigate on surfaces of arbitrary orientation. In order to overcome the gravitational force, such robots are equipped with adhesion devices with a travel surface. This direction in technology is relatively new, and requires fundamental research. One of the main tasks of designing such robots is the task of ensuring the robot's fixity on a vertical or other surface orientation at maximum technological loads. The importance of this task is explained by the fact that in carrying out manufacturing operations, technological loads are added to the weight of the mobile robot. To prevent an emergency, that is, the fall of the robot from the vertical displacement surface, it is necessary to find a rational relationship between the adhesion forces of the robot (friction forces) and its technological load, represented as the magnitude of the response to the applied technological load. These technological operations can include various production operations that have a force on the robot and, if they exceed their allowable values, can lead to the robot falling from the vertical displacement surface.

The proposed mathematical model allows creating graphs of changes in the technological reaction depending on the angle of inclination of the surface to move the robot to the horizon at given coefficients of friction of the grips of the robot. It is more accurate to set the dependencies as a function $N = f(\alpha,G,\mu)$, where: α is the angle of inclination of the robot's surface in relation to the horizon; G is the weight force of the robot; μ is the friction coefficient of the robot grips with the displacement surface.

Various designs of vertical movement robots have been proposed in [1–3], but in these researches there are no analytical models of dynamic loads of mobile robots. In the robot designs [4, 5], technical means of energy recuperation of the travel drives are offered, which allow to reduce the power of the drives, and hence the total mass of the robot. A model of motion of a robot with a glide seal is proposed in [6], which makes it possible to increase the force of adhesion of the robot with the travel surface, but only for vacuum grippers. The technical solution [7] also allows to increase the adhesion force of the robot due to adhesion. Researches [8] suggest a robot model for moving through trees, that is, on surfaces with a porous structure. In publications [9, 10], studies of the dynamics of mobile robots of traditional design, that is, robots that work only in the Cartesian coordinate system, are presented.

A dynamic model in the form of a state space is presented in [11], which allows increasing the productivity of the robot in terms of tracking the desired path, i.e. the trajectory of the robot. The movements of an anthropomorphic walking mobile robot are presented in [12]. This article proposes a method for calculating the muscles of a robot in the form of pneumatic chambers. These cameras allow the robot to move along an angular coordinate system, which is typical for humans. Also in the context of building a model of a walking robot, studies are of interest [13]. This paper proposes an analysis of four cases of robot preload in equilibrium, however, without taking into account the technological load.

Original technical solutions [14] for performing technological operations using a walking robot based on vacuum devices mounted on a tracked transmission are very promising for the industry. But this source does not present any research on the dynamics of the movement of the robot. Earlier, the dynamics of the walking mechanism was considered in [15], in which the passive two-legged mechanism was transformed into a 3D dynamic model of the walking device. In this article, the oscillations of the knee joint of a walking device were investigated. These studies are of undoubted interest for the construction of walking robots, however, they do not consider the tasks of calculating the parameters of dynamic loads in the context of the mobile robot performing technological operations. For the design of mobile robots of arbitrary orientation in the technological space, mathematical models can be recommended [16].

*CORRESPONDING AUTHOR | Mikhail Polishchuk | ✉ borchiv@ukr.net

An analysis of the above studies indicates the need to build a dynamic model of the robot, which not only takes into account the technological load, but also allows you to calculate the maximum permissible values of the specified load. Moreover, the maximum permissible technological load should be understood as the load at which the robot is held on the surface of movement. Therefore, the purpose of these studies is to obtain analytical formulas for calculating the allowable technological load from power operations performed by the robot in various fields of its application.

THE DESIGN OF THE WALKING ROBOT

Before proceeding with the presentation of the dynamic model, let us consider a fundamentally new construction of the robot and the sequence of its movement. In Figure 1 shows the position of the robot on a surface inclined to the horizon at angles $0 \leq \alpha \leq 180^0$ and $0 \leq \varphi \leq 180^0$. The robot has four legs, the construction of which is discussed below. The legs of the robot work in pairs on the diagonal of its body. In the initial position, the legs (pedipulators) 1 and 3 are bent under the different pressure in the hydraulic conduits, and their grippers 9 and 10 are engaged with the travel surface. Legs 2 and 4 are straightened and their grippers 7 and 8 are free of adhesion. The actuator 5 alternately serves legs 1 and 2 by switching the electromagnetic clutch, and the actuator 6 also alternately turns the legs 3 and 4. When the grippers 9 and 10 are adhered with the travel surface, the actuator 5 rotates the leg 1 about the axis "G" of the gripper 10, and the actuator 6 rotates the leg 3 around the "H" axis of the gripper 9. That's how the robot moves one step forward depending on the amount of the angle of rotation relative to these axes. When the grippers, for example, 7 and 8 are free of adhesion, drive 5 rotates leg 2 around axis "A" and at the same time drive 6 turns leg 4 around axis "B". Legs 2 and 4 are free from adhesion and are prepared for the next step. After the first step, the grippers 7 and 8 of these legs will be adhered with the travel surface and, under the influence of the same actuators 5 and 6, will rotate already around the gripper axes adhered to the travel surface [17].

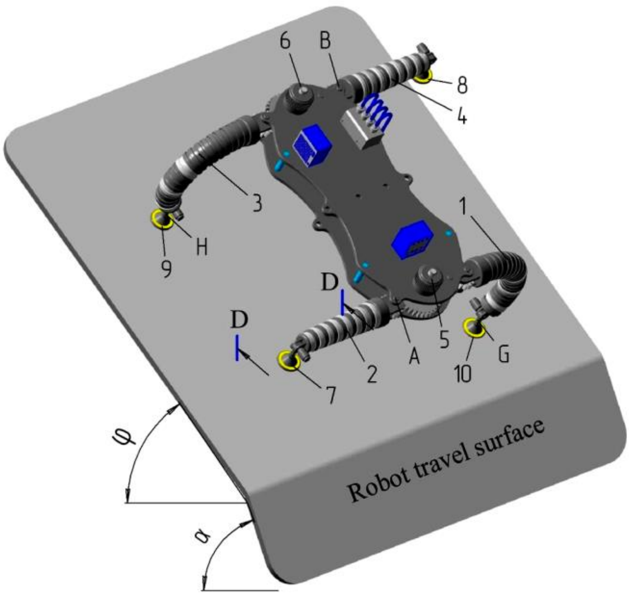

Figure 1. The robot's position on the travel surface inclined to the horizon.

To understand the robot legs mechanism on Figure 2, the longitudinal section D-D (Figure 1) of the foot of the pedipulator is shown. Each pedipulator is made in the form of a set of rings from the initial 11 to the last "n". The number of rings is determined by the purpose of the robot: the more rings, the higher the accuracy of the orientation of the pedipulators, and with a decrease in the number of rings, the robot's carrying capacity rises. All rings are compressed by an elastic stretch element 12 (for example, a cylindrical spring of tension) arranged along their axis and pivotally attached to the ring set-closing sleeves 13 and 14. In addition, corrugated conduits 15 and 16 are mounted inside the rings. These conduits are under different pressures gas or liquid. All the rings of legs of the robot come into contact with each other along the spherical outer 17 (Figure 2) and the inner surfaces 18 with radii R_i and R_{i+1}. The elastic element 12 is pivotally mounted on the axles 19 and 20, and the corrugated conduits 15 and 16 are fixed to the sleeves 13 and 14.

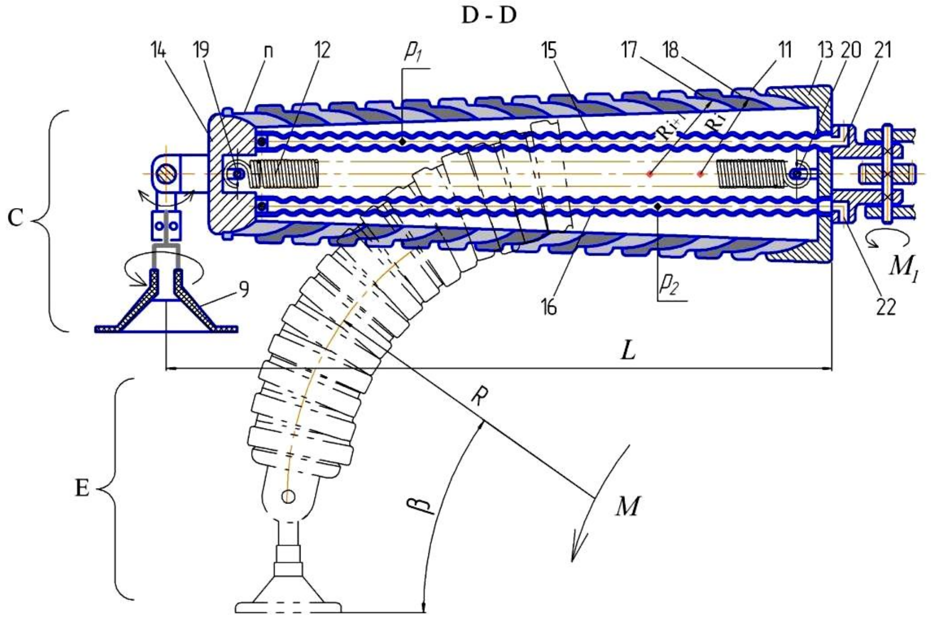

Figure 2. Mobile robot leg design.

These conduits have channels 21 and 22 for their connection to a hydraulic or pneumatic system. Due to the difference in pressure p_1 and p_2 in the conduits 15 and 16, the moment M of the bend of the robot's leg arises by an angle β of radius R (Figure 2):

$$M = \frac{\pi d^2}{4} e(p_1 - p_2) \tag{1}$$

where: d – internal diameter of the conduits; e is the eccentricity of the displacement of the axis of the conduits relative to the axis of the robot's leg. In this case, the value of the deformation ε of the robot's leg is:

$$\varepsilon = \frac{e}{R} = \frac{\beta e}{L} \tag{2}$$

If there is a pressure difference in conduits 15 and 16, the robot moves from position "C" to the bent position "E". Creating different combinations of pressures (p_1 - p_2), we get a different position of the robot's leg. Thus, the robot steps by two twisting moments: the leg M bending and the rotating torque M_1 from the motors 5 and 6 (Figure 1).

Table 1 shows the frames of the steps of moving the robot with a description of the movements of its legs. In the second column of the table, the image of the robot is shown in the plan view. Third column of the table gives descriptions of the state of the gripping devices of the robot for coupling with the vertical displacement surface. Also shows the movements that the legs of the robot perform: each pair of legs of the robot, located on the diagonal of the case, moves in turn with a periodic stop during the turn of the next pair of legs of the robot.

Table 1. Steps of moving the robot.

Step No	The position of the robot (plan view)	Explanation of robot movement
0	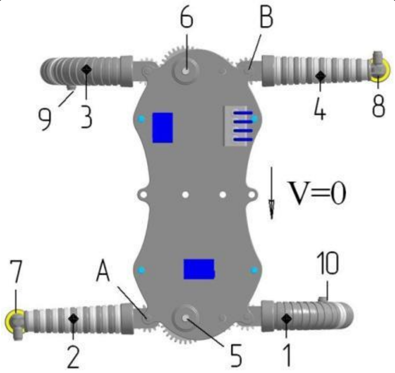	Starting position: Legs 1 and 3 are bent and adhered with the travel surface, grips 9 and 10 (along the diagonal of the robot's body). Legs 2 and 4 are straightened into a straight line. The grippers 7 and 8 are free of adhesion.

1	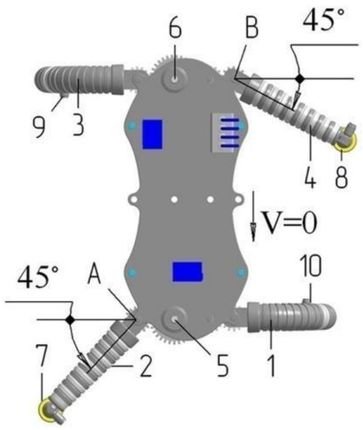	The robot does not move V=0 The rotation of the legs free of adhesion: the leg 2 by the actuator 5 is rotated around the point "A" and the leg 4 by the drive 6 - around the point "B" by an angle of 45°.
2	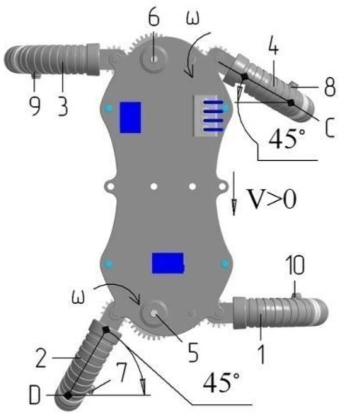	The beginning of the robot's movement. Legs 2 and 4 after rotation are bent and adhered to the travel surface by grippers 7 and 8. Legs 1 and 3 with grippers 10 and 9 are disengaged from the travel surface. The robot moves V> 0 by turning the legs 2 and 4 of the actuators 5 and 6 around the points D and C.
3	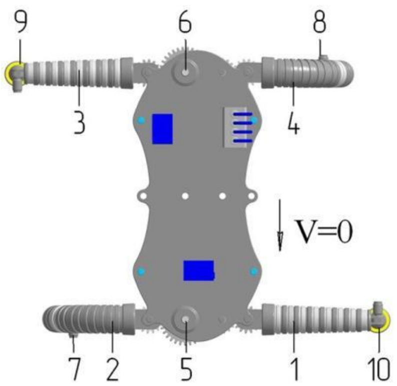	The robot moved one step by turning the legs 2 and 4 around the gripper axes 7 and 8. At the same time, the free legs 1 and 3 are straightened.
4	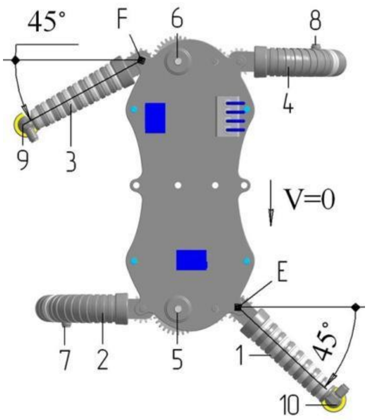	The robot does not move V=0 Turning legs 1 and 3 around points E and F, respectively, drives 5 and 6.

5	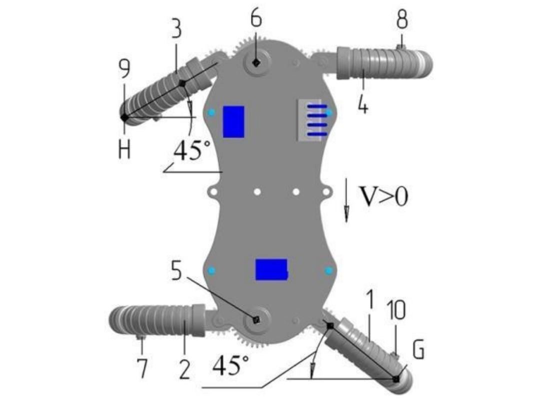	The beginning of the movement of the robot in the second step. Legs 1 and 3 are bent and adhere to the surface by movement of the grippers 10 and 9. Legs 2 and 4 are disengaged from the travel surface. The robot moves V> 0 by turning legs 1 and 3 by drives 5 and 6 around points G and H.
6	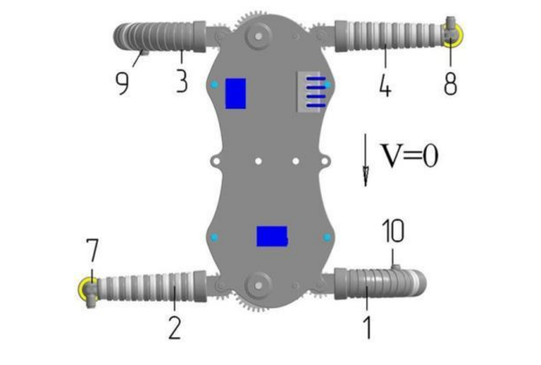	The robot moved one more step by turning the legs 1 and 3 around the gripper axes 10 and 9. At the same time straightening of legs 2 and 4 took place. The legs of the robot returned to their original position. Then the cycle of movement is repeated.

In this way, the movement of the robot occurs due to the rotation of each pair of legs (along the diagonal of the body) around the axes of the adhered grips. One engine alternately serves a pair of legs, due to the switching of the electromagnetic clutch, because the legs also turn in turn.

Figure 3 shows examples of different positions in the space of a mobile robot, which has six legs for increased patency over complex surfaces. So in Figure 3(a), the front pair of legs overcomes the elevation h_1, the central (middle) pair is a hollow h_2, and the rear pair of legs is the elevation h_3 of the relief of the travel surface. In Figure 3(b) the robot overcomes a niche with depth L and height H when moving along a vertical wall. In Figure 3(c) shows the transition of the robot from the wall surface to the ceiling.

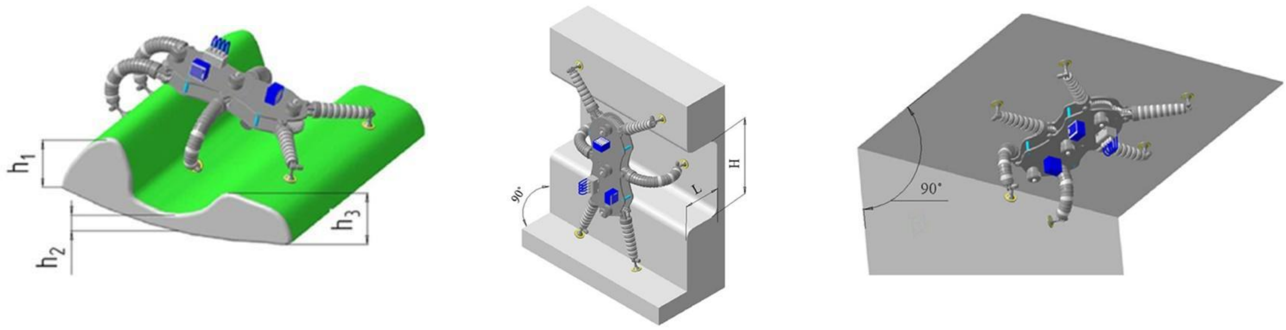

(a) (b) (c)

Figure 3. Options of the position of the mobile robot when moving on surfaces of arbitrary orientation.

DETERMINATION OF THE ALLOWABLE TECHNOLOGICAL LOAD OF THE ROBOT

Here, the allowable technological load is the allowable effort of the technological operation, which excludes the fall of the robot from a vertical surface. In Figure 4, the technological load is represented as the force of its reaction N, which consists of the efforts of the reactions N_1, N_2 at the points of contact of the gripping devices with the surface on which the robot moves. These technological operations may include various manufacturing operations, for example, such as: drilling, riveting, and installing fasteners and dowels, cutting metal structures, as well as similar technological impacts on the service object.

Let the right hind leg 1 (Figure 4) bear on a plane that is inclined to the horizontal plane at an angle α, and the left front leg 2 lean on a plane that is inclined at an angle φ, and the intersection line of these planes is horizontal. The axis of symmetry of the robot forms an angle ψ with the first plane. We choose the origin of the coordinate system 0_{xyz} at the point of contact of the foot 1 with the plane. The 0_x axis is parallel to the intersection of the planes, the 0_z axis is perpendicular to the first bearing plane, the 0y axis is perpendicular to the two previous axes. Such forces act on the robot (Figure 4): the weight force G is applied at the centre of the weight of the robot and is directed vertically downwards. The technological reaction N is applied at the centre of the weight and is directed perpendicular to the plane of the robot body; the adhesion forces Q_{1n} and Q_{2n} of the legs with the travel surface are directed along the normal's to the planes. Normal reactions N_1 and N_2, are directed opposite to the forces of adhesion. The frictional forces Q_{1T} and Q_{2T} lie in the corresponding planes. Since the magnitude of the frictional forces Q_{1T} and Q_{2T} and their direction are unknown, we decompose each of them into two components Q_{1T} (Q_{1x}, Q_{1y}), Q_{2T} (Q_{2x}, Q_{2y}), one of which is parallel to the 0x axis, and the second is perpendicular to this axis and lies in corresponding to the plane. In addition, the torques M bend the legs of the robot, and the moments M_1 rotate them around the gripper axles with which the robot is held on the travel surface.

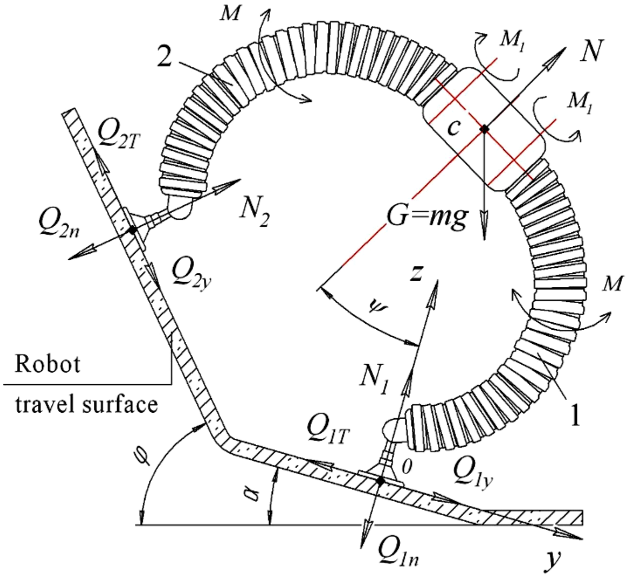

Figure 4. The scheme of forces acting on the robot.

The robot, under the influence of this arbitrary spatial force system, is in equilibrium, and therefore six equilibrium conditions must be fulfilled, namely: the algebraic sum of the projections of all forces on each of the coordinate axes equals zero:

$$\sum_{i=1}^{n} F_{ix} = 0; \quad Q_{1x} + Q_{2x} = 0 \tag{3}$$

$$\sum_{i=1}^{n} F_{iy} = 0; \quad Q_{1y} + Q_{2y}\cos(\varphi-\alpha) + \mathrm{N}\sin\psi + (\mathrm{Q}_{2n} - \mathrm{N}_2)\sin(\varphi-\alpha) + \mathrm{G}\sin\alpha = 0 \tag{4}$$

where: G is the force of gravity, $G=mg$ (m is the mass of the robot; g is the acceleration of gravity, g = 9.8 m/c^2.

$$\sum_{i=1}^{n} F_{iz} = 0; \quad N_1 - Q_{1n} + Q_{2y}\sin(\varphi-\alpha) + \mathrm{N}\cos\psi - (\mathrm{Q}_{2n} - \mathrm{N}_2)\cos(\varphi-\alpha) - \mathrm{G}\cos\alpha = 0 \tag{5}$$

The algebraic sum of the moments of all forces relative to each of the coordinate axes must also be zero:

$$\left\{\begin{aligned} &\sum_{i=1}^{n} M_{ix} = 0; \quad \begin{aligned}&(\mathrm{N}_2 - \mathrm{Q}_{2n})\cos(\varphi-\alpha)\,\mathrm{y}_2 + (\mathrm{N}_2 - \mathrm{Q}_{2n})\sin(\varphi-\alpha)\,\mathrm{z}_2 - \mathrm{Q}_{2y}\cos(\varphi-\alpha)\,\mathrm{z}_2\\ &+\mathrm{Q}_{2y})\sin(\varphi-\alpha)\,\mathrm{y}_2 - G\cos\alpha\, y_c + G\sin\alpha\, z_c + N\cos\psi\, y_c + N\sin\psi\, z_c = 0\end{aligned}\\ &\sum_{i=1}^{n} M_{iy} = 0; \quad (\mathrm{Q}_{2n} - \mathrm{N}_2)\cos(\varphi-\alpha)\,\mathrm{x}_2 + \mathrm{Q}_{2x}\,\mathrm{z}_2 + G\cos\alpha\, x_c - N\cos\psi\, x_c = 0\\ &\sum_{i=1}^{n} M_{iz} = 0; \quad (\mathrm{Q}_{2n} - \mathrm{N}_2)\sin(\varphi-\alpha)\,\mathrm{x}_2 - \mathrm{Q}_{2x}\, y_2 - G\sin\alpha\, x_c - N\sin\psi\, x_c + Q_{2y}\cos(\varphi-\alpha)\,\mathrm{x}_2 = 0 \end{aligned}\right. \tag{6}$$

where, x_2, y_2, z_2 – coordinates of the point of contact with the plane of the second leg; x_c, y_c, z_c – are the coordinates of the center of the weight of the robot.

In the system of Equation. (6), from the last two equations we exclude the unknown frictional force Q_{2x} and we get a system of two equations with two unknowns:

$$
\begin{aligned}
(\mathrm{N}_2 - \mathrm{Q}_2)\mathrm{a}_1 + Q_{2y}a_2 = Gb_1 + Nb_2 \\
(\mathrm{N}_2 - \mathrm{Q}_2)\mathrm{c}_1 + Q_{2y}c_2 = Gb_2 + Nb_4
\end{aligned}
\tag{7}
$$

where:

$a_1 = -x_2(\mathrm{y}_2\cos(\varphi-\alpha) + \mathrm{z}_2\sin(\varphi-\alpha))$; $a_2 = x_2 z_2 \cos(\varphi-\alpha)$;

$c_1 = \mathrm{y}_2\cos(\varphi-\alpha) + \mathrm{z}_2\sin(\varphi-\alpha)$; $c_2 = \mathrm{y}_2\sin(\varphi-\alpha) - \mathrm{z}_2\cos(\varphi-\alpha)$;

$b_1 = x_c(\mathrm{z}_2\sin\alpha - \mathrm{y}_2\cos\alpha)$; $b_2 = x_c(\mathrm{z}_2\sin\psi + \mathrm{y}_2\cos\psi)$;

$b_3 = \mathrm{y}_c\cos\alpha - \mathrm{z}_c\sin\alpha$; $b_4 = -\mathrm{y}_c\cos\psi - \mathrm{z}_c\sin\psi$.

Solving the system of Equation. (7), we get:

$$N_2 = Q_2 + Gd_1 - Nd_2;\quad Q_{2y} = Gd_3 + Nd_4 \tag{8}$$

where:

$\Delta = a_1c_2 - c_1a_2$;

$d_1 = \dfrac{b_1c_2 - b_3a_2}{\Delta}$;

$d_2 = -\dfrac{b_2c_2 - b_4a_2}{\Delta}$;

$d_3 = \dfrac{b_3a_1 - b_1c_1}{\Delta}$;

$d_4 = \dfrac{b_4a_1 - b_2c_1}{\Delta}$.

Considering expression (4), from the last system of Equation. (6) we determine the component of the frictional force Q_{2x}:

$$Q_{2x} = Gh_1 + Nh_2 \tag{9}$$

in which:

$h_1 = (\mathrm{x}_2(\mathrm{d}_3\cos(\varphi-\alpha) - \mathrm{d}_1\sin(\varphi-\alpha)) - \mathrm{x}_c\sin\alpha)/\mathrm{y}_2$;

$h_2 = (\mathrm{x}_2(\mathrm{d}_4\cos(\varphi-\alpha) + \mathrm{d}_2\sin(\varphi-\alpha)) - \mathrm{x}_c\sin\psi)/\mathrm{y}_2$.

Further, from the system of Equation. (4), we find other unknown normal reactions and friction forces:

$$N_1 = Q_1 + Gh_3 - Nh_4;\qquad Q_{1y} = Gh_5 + \mathrm{N}h_6;\qquad Q_{1x} = -Q_{2x} \tag{10}$$

where the designations for compact notation is:

$h_3 = \cos\alpha - \mathrm{d}_1\cos(\varphi-\alpha) - \mathrm{d}_3\sin(\varphi-\alpha)$;

$h_4 = \cos\psi - \mathrm{d}_2\cos(\varphi-\alpha) + \mathrm{d}_4\sin(\varphi-\alpha)$;

$h_5 = \sin\alpha - \mathrm{d}_3\cos(\varphi-\alpha) + \mathrm{d}_1\sin(\varphi-\alpha)$;

$h_6 = \sin\psi - \mathrm{d}_4\cos(\varphi-\alpha) - \mathrm{d}_2\sin(\varphi-\alpha)$.

The total frictional forces for each leg should not exceed the limit values, and the normal forces $(Gh_1+Nh_2)^2+(Gh_5+Nh_6)^2 \leq \mu^2(Q_1+Gh_3-Nh_4)^2$ and force responses are positive, that is

$$Q_{1T}=\sqrt{Q_{1x}^2+Q_{1y}^2}\leq \mu N_1;$$
$$N_1>0;$$
$$Q_{2T}=\sqrt{Q_{2x}^2+Q_{2y}^2}\leq \mu N_2;$$
$$N_2>0. \tag{11}$$

We substitute expressions for the force responses into Equation. (11) and solve inequalities relatively to the reaction N of the technological load of the robot:

$$N_1>0\Rightarrow N<\frac{Q_1+G(\cos\alpha-\mathrm{d}_1\cos(\varphi-\alpha)-\mathrm{d}_3\sin(\varphi-\alpha))}{(\cos\psi-\mathrm{d}_2\cos(\varphi-\alpha)+\mathrm{d}_4\sin(\varphi-\alpha))};$$
$$N_2>0\Rightarrow N<\frac{Q_2+Gd_1}{d_2};$$
$$(\mathrm{Gh}_1+\mathrm{Nh}_2)^2+(\mathrm{Gh}_5+\mathrm{Nh}_6)^2\leq\mu^2(\mathrm{Q}_1+\mathrm{Gh}_3-\mathrm{Nh}_4)^2;$$
$$(\mathrm{Gh}_1+\mathrm{Nh}_2)^2+(\mathrm{Gd}_3+\mathrm{Nd}_4)^2\leq\mu^2(\mathrm{Q}_2+\mathrm{Gd}_1-\mathrm{Nd}_2)^2. \tag{12}$$

In the last two inequalities, similar elements are grouped, and as a result, square inequalities:

$$u_1N^2+2u_2N+u_3\leq 0;\quad u_4N^2+2u_5N+u_6\leq 0, \tag{13}$$

where,

$$u_1=\mathrm{h}_2{}^2+\mathrm{h}_6{}^2-\mu^2\,\mathrm{h}_4{}^2;\quad \mathrm{u}_2=\mathrm{G}(\mathrm{h}_1\mathrm{h}_2+\mathrm{h}_5\mathrm{h}_6)+\mu^2(\mathrm{Q}_1+\mathrm{Gh}_3)\,\mathrm{h}_4;$$
$$\mathrm{u}_3=(\mathrm{Gh}_1)^2+(\mathrm{Gh}_5)^2-\mu^2(\mathrm{Q}_1+\mathrm{Gh}_3)^2;$$
$$\mathrm{u}_4=\mathrm{h}_2{}^2+\mathrm{d}_4{}^2-\mu^2\,\mathrm{d}_2{}^2;\quad \mathrm{u}_5=\mathrm{G}(\mathrm{h}_1\mathrm{h}_2+\mathrm{d}_3\mathrm{d}_4)+\mu^2(\mathrm{Q}_2+\mathrm{Gd}_1)\,\mathrm{d}_2;$$
$$\mathrm{u}_6=(\mathrm{Gh}_1)^2+(\mathrm{Gd}_3)^2-\mu^2(\mathrm{Q}_2+\mathrm{Gd}_1)^2.$$

After solving inequalities (13), we get ranges of numerical values of the robot workload force:

$$0<N\leq\frac{-u_2+\sqrt{u_2^2-u_1u_3}}{u_1};\quad 0<N\leq\frac{-u_5+\sqrt{u_5^2-u_4u_6}}{u_4}. \tag{14}$$

Among the values of the reaction force N, calculated from Equation. (12) and (14), choose a larger value that simultaneously satisfies all the inequalities. Thus, we determine the intervals of change of the allowable technological load of the walking robot. And here the technological load is determined by the reaction of its force N within acceptable limits Equation. (14), more precisely the reaction of the effort of the technological operation, which is performed by a mobile robot.

PROGRAMMING THE COORDINATES OF THE MOVEMENT OF THE ROBOT

To make a control program for the walking robot, it is necessary to find the equations by which the coordinates of the characteristic displacement points can be calculated. Suppose that the fulcrum of the hind leg is remote from the line of intersection of the planes of the travel surface by the amount a_{11}. Then, by the cosine theorem, one can find the distance a_{22} of the fulcrum of the front leg from the indicated line of displacement

$$a_{11}^2+a_{22}^2+2a_{11}a_{22}\cos(\varphi-\alpha)=(2\,\mathrm{a})^2 \tag{15}$$

where a – is the distance along the robot axis from the center of gravity to the attachment point to the robot body. Then from Equation. (15) find the distance a_{22} of the fulcrum of the robot's leg:

$$a_{22} = \sqrt{4a^2 - a_{11}^2 \sin^2(\varphi - \alpha)} - a_{11}\cos(\varphi - \alpha) \tag{16}$$

In this way, the coordinates of the fulcrum of the front leg relative to the selected coordinate reference system will be:

$$\begin{gathered} x_2 = 2R_0 \sin\beta_0 \sin 45^o + 2b_1 \\ y_2 = a_{11} + a_{22}\cos(\varphi - \alpha); \quad z_2 = a_{22}\sin(\varphi - \alpha) \end{gathered} \tag{17}$$

where, $2b_1$ – the width of the robot design in the place where the legs are attached; β_0 – is the initial angle of the leg bend; the initial radius of the leg bend R_0 =L/ β_0. It must be remembered that the last two parameters are determined by the differences in pressures ($p_1 - p_2$) of gas or liquid in flexible conduits 15 and 16 (look Figure 2) robot legs.

The angle ψ of the inclination of the central axis of the robot to the coordinate plane is calculated from formula

$$\psi = \arcsin\left(\frac{(\mathrm{a}_{22} - \mathrm{R}_0 \sin\beta_0 \sin 45^o \,\mathrm{tg}(45^o - \varphi_1)\sin(\varphi - \alpha) + \mathrm{h}(\cos(\varphi - \alpha) - 1)}{2a}\right) \tag{18}$$

where, during movement, depending on the topology of the travel surface, the angle φ_1 can vary within the limits $0 \le \varphi_1 \le 90°$; h = R - Rcos β; R = L/β. The angle β of the bending of the robot feet is found from equation:

$$\frac{\sin\beta}{\beta} = \frac{\sin\beta_0 \sin 45^o}{\beta_0 \cos(45^o - \varphi_1)} \tag{19}$$

An approximate solution of this equation, which determines the angle β of bending the robot's legs, looks as follows:

$$\beta = \sqrt{10 - \sqrt{100 - 120\left(1 - \frac{\sin\beta_0 \sin 45^o}{\beta_0 \cos(45^o - \varphi_1)}\right)}} \tag{20}$$

Now we can find the coordinates of the center of the robot's weight, which, when the robot is controlled, will be processed by its digital reason:

$$\begin{gathered} x_c = R_0 \sin\beta_0 \sin 45^o + b_1 \\ y_c = a\cos\psi - R_0 \sin\beta_0 \sin 45^o tg(45^o - \varphi_1) \\ z_c = R(1 - \cos\beta) + a\sin\psi \end{gathered} \tag{21}$$

DETERMINATION OF THE ROBOT'S FORCES DURING THE EXECUTION OF THE TECHNOLOGICAL OPERATION

Unlike the mode of moving a robot, when it moves with each pair of legs alternately, while performing technological operations, the robot does not move and stands on four legs. Then, in the general case, four normal reactions and four friction forces occurs, the directions of which are unknown, that is, the problem is statically indeterminate. This is explained by the fact that it is possible to compose six equations of equilibrium, and there are twelve parameters which is unknown in this case. However, the problem can be made statically determined if we assume that certain conditions are fulfilled, namely:

- when carrying out the technological operation, the foot fulcrum are placed symmetrically with the vertical symmetry plane of the robot;
- the external forces of adhesion Q, the weight of the robot G and the reaction of the technological load N lie in this plane or are parallel to the plane of symmetry of the robot;
- the reactions in the symmetrically placed legs are identical and also parallel to the symmetry plane of the robot body;
- since are interested in the maximum value of the technological reaction N, we assume that in one of the pairs of legs (where a smaller normal reaction), the frictional force reaches its limiting value.

Then, considering the above limitations, we can form three equilibrium equations, which include only three unknowns, namely:

$$\begin{cases} \sum_{i=1}^{n} F_{iy} = 0;\ 2Q_{1y} + 2\mu N_2 \cos(\varphi-\alpha) - \mathrm{N}\sin\psi + 2(\mathrm{Q}_{2n} - \mathrm{N}_2)\sin(\varphi-\alpha) - \mathrm{G}\sin\alpha = 0; \\ \sum_{i=1}^{n} F_{iz} = 0;\ 2N_1 - 2Q_{1n} + 2\mu N_2 \sin(\varphi-\alpha) + \mathrm{N}\cos\psi - 2(\mathrm{Q}_{2n} - \mathrm{N}_2)\cos(\varphi-\alpha) - \mathrm{G}\cos\alpha = 0; \\ \sum_{i=1}^{n} M_{ix} = 0; \\ 2(\mathrm{N}_2 - \mathrm{Q}_{2n})(\cos(\varphi-\alpha)\,\mathrm{y}_2 + \sin(\varphi-\alpha)\,\mathrm{z}_2) - 2\mu N_2(\cos(\varphi-\alpha)\,\mathrm{z}_2 - \sin(\varphi-\alpha)\,\mathrm{y}_2) - \\ -G\cos\alpha y_c + G\sin\alpha z_c + N\cos\psi y_c + N\sin\psi z_c = 0. \end{cases} \tag{22}$$

From the last equation we find the component reaction N_2

$$N_2 = a_{12}Q_{2n} + b_{12}G - c_{12}N \tag{23}$$

where,

$$\Delta_1 = 2(\cos(\varphi-\alpha)\,\mathrm{y}_2 + \sin(\varphi-\alpha)\,\mathrm{z}_2) - 2\mu(\cos(\varphi-\alpha)\,\mathrm{z}_2 - \sin(\varphi-\alpha)\,\mathrm{y}_2);$$

$$a_{12} = \frac{2(\cos(\varphi-\alpha)\,\mathrm{y}_2 + \sin(\varphi-\alpha)\,\mathrm{z}_2)}{\Delta_1};$$

$$b_{12} = \frac{\cos\alpha y_c - \sin\alpha z_c}{\Delta_1};$$

$$c_{12} = \frac{\cos\psi y_c + \sin\psi z_c}{\Delta_1}.$$

Further from the first two equations we find the friction force Q_{1y} and normal reaction N_1

$$Q_{1y} = Q_{2n}(\mathrm{d}_{12}\mathrm{a}_{12} - \sin(\varphi-\alpha)) + \mathrm{G}(\mathrm{d}_{12}\, b_{12} + \frac{1}{2}\sin\alpha) - \mathrm{N}(\mathrm{d}_{12}\, c_{12} - \frac{1}{2}\sin\psi);$$
$$N_1 = Q_{1n} + Q_{2n}(\mathrm{h}_{12}\mathrm{a}_{12} + \cos(\varphi-\alpha)) + \mathrm{G}(\mathrm{h}_{12}\, b_{12} + \frac{1}{2}\cos\alpha) - \mathrm{N}(\mathrm{h}_{12}\, c_{12} + \frac{1}{2}\cos\psi); \tag{24}$$

where, $d_{12} = \sin(\varphi-\alpha) - \mu\cos(\varphi-\alpha)$; $h_{12} = -\mu\sin(\varphi-\alpha) - \cos(\varphi-\alpha)$

The reaction N_2 is positive, and therefore the maximum value of the technological reaction should not exceed the next value

$$N_2 > 0 \quad \Rightarrow \quad N < \frac{Q_{2n}a_{12} + Gb_{12}}{c_{12}} \tag{25}$$

In addition, the frictional force Q_{1y} must not exceed the limit value

$$Q_{1y} < \mu N_1 \quad \Rightarrow \quad N < \frac{\mu N_3 - Q_3}{\mu(\mathrm{h}_{12}\mathrm{c}_{12} + 0.5\cos\psi) - (\mathrm{d}_{12}\mathrm{c}_{12} - 0.5\sin\psi)} \tag{26}$$

where the normal reaction of the force of the technological load and the friction force will be:

$$N_3 = Q_{1n} + Q_{2n}(\mathrm{h}_{12}\mathrm{a}_{12} + \cos(\varphi - \alpha)) + \mathrm{G}(\mathrm{h}_{12}\, b_{12} + \frac{1}{2}\cos\alpha);$$
$$Q_3 = Q_{2n}(\mathrm{d}_{12}\mathrm{a}_{12} - \sin(\varphi - \alpha)) + \mathrm{G}(\mathrm{d}_{12}\, b_{12} + \frac{1}{2}\sin\alpha) \tag{27}$$

In this way, the task of finding the forces of the technological load becomes statically determined for three typical positions of the robot in space, namely:

- the robot is on the floor, then it is necessary to substitute in the above formulas the values $\varphi=0^0$, $\alpha=0^0$;
- if the robot is on the ceiling, then you need to substitute in the above formulas $\varphi=180^0$, $\alpha=180^0$;
- when the robot is on a vertical wall, then it is necessary to substitute in the above formulas the values $\varphi=90^0$, $\alpha=90^0$.

The developed analytical model of the robot allows you to design it with a forecast of the permissible technological load, which is determined by the intervals of values of the normal reactions of forces (25) and (26). Here, the permissible technological load should be understood as the load at which the fall of the robot from the vertical surface of its movement is excluded.

RESULTS OF MODELING

Actualization of the robot's behavior simulation at different angles of inclination to the horizon and the magnitude of the adhesion of the robot grips with the travel surface made it possible to establish the following. Figure 5 shows the graphs of the dependence of the technological load on the angle of inclination of the travel surface of the robot, when only four of its legs are on the same surface. Curves 1 and 2 show the state when the hind leg (1) and the front leg (2) do not detach from the travel surface, and curve 3 characterizes the state of the robot when it moves, but the grips of its legs do not slip over the travel surface. All three robot motion states exclude the possibility of an emergency, i.e. fall down robot from the travel surface. As we can see from the graphs, an increase of the friction coefficient of the robot grips with the travel surface from the value μ = 0.2 (Figure 5(a)) to μ = 0.5 (Figure 5(b)), namely by 40%, leads to the possibility of increasing the minimum technological load N from 350 (N) to 770 (N), i.e. by 45.5%. This effect is evidenced by the dominant influence of adhesion force on the increase in the technological load of the robot.

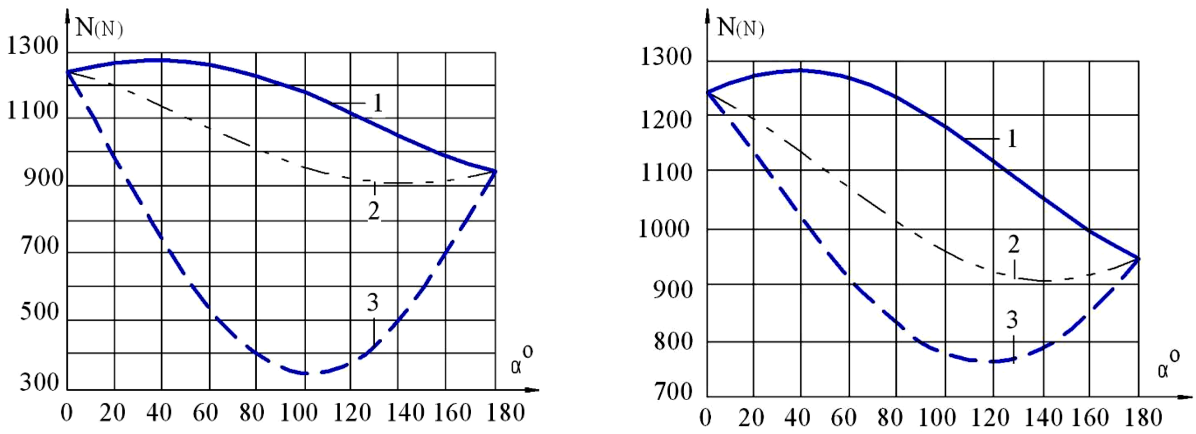

(a) (b)

Figure 5. Graphs of technological reaction change $N = f(\alpha)$ depending on the robot travel surface inclination angle α to the horizon at a friction coefficient of the robot grips: (a) μ = 0.2 and (b) μ = 0.5.

In the graph of Figure 6 shows the dependence of the technological load on the angle of inclination of the robot travel surface, when the travel surfaces are not only at an angle to the horizon, but the feet themselves are located on different surfaces, in particular at an angle $\varphi - \alpha$ = 30°.

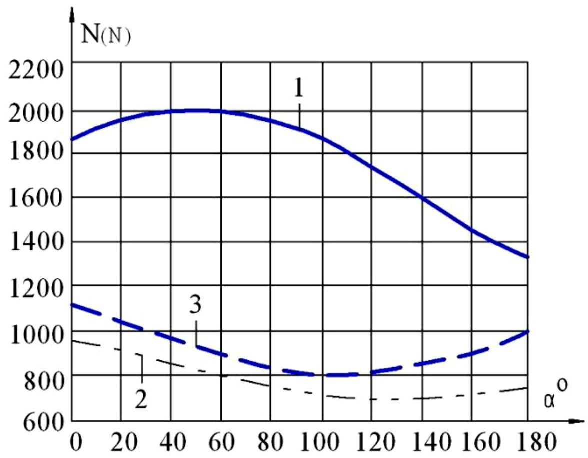

Figure 6. Graphs of technological reaction change $N = f(\alpha)$ with the difference in the slope of the surfaces on which the robot legs rest $\varphi - \alpha = 30°$ and with a friction coefficient of the robot grips $\mu = 0.5$.

Here arises the effect of the convergence of states (2) and (3), namely, when the front leg of the robot does not detach from the travel surface, and the hind leg, diagonally disposed on the robot body, moves without sliding. Obviously, reaching the maximum technological load corresponds to state (1), when the robot does not move. Therefore, it can be recommended to use the robot in motion when performing light load operations, such as video shooting, diagnostics of the surface condition of hydraulic power plants, monitoring of large conduits and various industrial mines, and for performing technological operations such as applying special coatings to objects and welding operations. At the same time, the execution of operations with a large technological load should be carried out in a stationary state of the mobile robot.

CONCLUSIONS

A fundamentally new design of the walking robot with flexible pedipulators - walking mechanisms, makes it possible to perform various technological and transport operations in any production space. The specified technological operations are such production tasks as drilling, installing dowels and rivets, cutting metal or concrete structures, as well as other technological loads in the form of a force effect on the robot.

The developed mathematical model makes it possible to calculate the possible technological load for a walking mobile robot with an arbitrary orientation of the displacement surface, namely, in the range of the inclination of the movement surface to the horizon from 0° to 180°. The system of equations for determining the coordinates of the movement of the legs of the robot and its center of gravity is recommended as a mathematical tool for programming the trajectory of the robot, taking into account technological loads.

REFERENCES

[1] Dethe DR, Jaju SB. Developments in wall climbing robots: a review. International journal of engineering research and general science. 2014; 2(3): 36–37.

[2] Apostolescu TC, Udrea C, Duminica D, Ionascu G, Bogatu I, Cartal LA, et al. Development of a climbing robot with vacuum attachment cups. Mechanical engineering and new high-tech products development. 2011;3: 258–267.

[3] Polishchuk MN, Tkach MM. Grip of walking robot. Patent UA 117979 IPC B65H 5/08.; Published Jul 10. 2017; 13: 4–6.

[4] Yampolskiy LS, Polishchuk MN, Persikov VK. Method and device for movement of pedipulators of walking robot. UA, Patent 111021. 2016; 4: 3–4.

[5] Polyshchuk MN. Pedipulator of robot of the vertical moving with possibility. Adaptive automatic control systems. 2016; 1(28): 107–115.

[6] Chashchukhin VG. Investigation of the movement parameters of a robot with a sliding seal. Bulletin of the Nizhny Novgorod University. 2011; 4 (2): 347–349.

[7] Silva M, Machado TJ. A survey of technologies and applications for climbing robots locomotion and adhesion. Instituto Superior de Engenharia do Porto Portugal. 2012.

[8] Lam TL, Xu Y. Tree climbing robot: Design, kinematics and motion planning. Springer Heidelberg New York 2012; 37–46.

[9] Dyshenko VS. Research of the dynamics of a mobile robot for moving along vertical surfaces: Dissertation. Candidate of Engineering Sciences. Kursk State Technical University. 2006; 108–105.

[10] Yehya M, Hussain S, Wasim A, Jahanzaib M, Abdalla H. A cost effective and light weight unipolar electroadhesion pad technology for adhesion mechanism of wall climbing robot. International Journal of Robotics and Mechatronics. 2014; 2(1): 4–10.

[11] Inel F, Babesse S. Adaptive sliding mode control of a novel cable driven robot model. Journal of Mechanical Engineering and Sciences. 2019; 13(2): 5150–5162.

[12] Polishchuk M, Tkach M. Mobile robot with an anthropomorphic walking device: Design and simulation. FME Transactions. 2020; 48(1): 13–20.

[13] Fernini B, Temmar M, Noor MM. Toward a dynamic analysis of bipedal robots inspired by human leg muscles. Journal of Mechanical Engineering and Sciences. 2018; 12(2): 3593-3604.

[14] Robotic system of Swiss firm Gekko Serbot AG. URL: https://www.designworldonline.com/cleaning-solar-panels-with-a-robotic-gecko/ (date of site visit: 09.02.2019).

[15] Kinugasa T, Ando K, Fujimoto S, Yoshida K, Iribe M. Development of a three-dimensional dynamic biped walking via the oscillation of telescopic knee joint and its gait analysis. Journal of Mechanical Engineering and Sciences. 2015; 9: 1529-1537.

[16] Polishchuk MN, Oliinyk VV. Dynamic model of a stepping robot for arbitrarily oriented surfaces. In: Hu Z., Petoukhov S, Dychka I, He M, (eds) Advances in Computer Science for Engineering and Education II. ICCSEEA Advances in Intelligent Systems and Computing, Springer, Cham. 2020;938: 32–42.

[17] Walking mobile robot: Patent UA No. 117065: Ukraine: Int. Cl. B62D 57/032. Appl. No a 2017 01440; Filed: 16.02.2017; Date of Patent: 11.06.2018; 11: 4–6.